Robust Model Predictive Control for Humanoids Standing Balancing

Robust Model Predictive Control for Humanoids Standing Balancing

Juan A. Castano, Chengxu Zhou, Zhibin Li, Nikos Tsagarakis

Abstract— **This paper presents the implementations of Model Predictive Control for the standing balance control of a humanoid to reject external disturbances. The strategies allow the robot to have a compliant behaviour against external forces resulting in a stable and smooth response. The first, ZMP based controller, compensates for the center of mass deviation while the second, attitude controller, regulates the orientation of the body to counterbalance the external disturbances. These two control strategies are combined as an integrated stabilizer, which further increases the effectiveness. Simulation studies on the COMAN humanoid are presented and the data are analysed. The simulations show significant improvements in rejection of external disturbances compared to an existing compliant stabilizer.**

I. INTRODUCTION

Control techniques that allow biped robots to reject external forces such as pushes are a fundamental prerequisite for the integration of humanoids in environments designed for humans. In particular, it is desired to have a natural and safe interaction of the robot with the environment, such that the robot is able to damp the energy added to the system by interactions [1]. To this aim, the stability and balance controls should be adaptive and continuously regulated according to the robot's state providing a soft yet reliable response against external forces. In this paper, the Center of Mass (CoM) states, namely the position and velocity, and the angular position and velocity (from IMU measurements) are used in two different balancing strategies which effectively reject external disturbances by providing a compliant response of the biped. Coupling of the individual strategies is considered and compensated, providing a cooperative behaviour.

Different works on balancing strategies have studied the bipedal balancing problem from different perspectives, for instance [2]–[4], among others, that provide different perspectives to cope with the robot balancing problem in presence of external disturbances. In [5], a balancing controller that combines strategies of ankle and hip bending is used. Stability is guaranteed using the Center of Pressure (CoP) principle. The control applies a torque at the ankles so that the biped absorbs the forces caused by an external push. This torque compensates the CoP disturbance, driving the biped to the stable position. In addition, authors consider the hip strategy, consisting of the bending of the body to change the CoM position and to keep the CoP inside the desired margins. The paper proposed to model the biped as a planar double inverted pendulum and used an integral LQR controller. Simulations on planar robot model were presented.

A controller that allows a soft transition between ankle and hip strategies is proposed in [3]. The works in [6], [7] present balancing controllers which are based on the linear inverted pendulum and double inverted pendulum respectively, with both models using a virtual spring damper to generate a compliant response of the system. The strategies use PD controllers and consider the CoP as stability principle. The control that makes the transition uses a proportional gain and considers a spline function to provide a smooth response.

In [8], a balancing strategy based on the center of gravity and Zero Moment Point (ZMP) is presented. The method allows the robot to keep balance using the simple inverted pendulum and by constraining the ZMP to the stability region [9]. The ZMP is a concept that has been presented in different works [10]. According to [11], the ZMP is the point in which the different ground forces affecting the body can be represented by a single one. While the ZMP remains inside the support polygon of the biped, it will not tip around the stance foot [12].

In our work, two balancing strategies are presented. The first one uses the cart-table model to provide a ZMP based response of the system, that generates a horizontal displacement of the CoM to reject the external disturbance while the ZMP is contained in the stability region. The second one is a rotation strategy based on the double integrator model. It is used to generate a rotational attitude control that absorbs external disturbances by rotating the upper body of the biped. The proposed strategies are coupled and, according to the applied disturbance, naturally respond with an ankle like strategy or a hip like strategy, providing a human like response. The desired translational and rotational references are mapped to the joint level by means of inverse kinematics.

The paper is organized as follows. Section II introduces the robust implementation of the Extended Prediction Self-Adaptive Control (EPSAC), which is used in the present work. The EPSAC control considers the disturbance frequency band, increasing the performance of the overall system. In Section III, two balancing strategies are presented and the compensation strategy to achieve a cooperative behaviour is presented. A simulation study is presented in Section IV, using a 3D model of the COmpliant huMANoid platform COMAN, built in the physics based simulator Open Dynamics Engine (ODE). Finally, conclusions are given in Section V.

This work is supported by the FP7 European project WALK-MAN (ICT-2013-10).

The authors are with the Department of Advanced Robotics, Istituto Italiano di Tecnologia, via Morego 30, 16163 Genova, Italy
Email: juan.castano@iit.it

II. Robust MPC Controller

MPC is a designation for controllers that uses a model of the plant to be controlled to obtain a control effort that minimizes an objective function over a time horizon. In this contribution, the Extended Prediction Self-Adaptive control (EPSAC) algorithm [13] has been selected since it allows multiple format choices to represent the system and includes a noise observer. The generic process model of the EPSAC algorithm is given by

$$y(t) = \Psi(t) + n(t)\,, \tag{1}$$

where $y(t)$ is the measured output of the process, $\Psi(t)$ is the model output and $n(t)$ is the process disturbance at discrete-time index t. The disturbance $n(t)$ can be modelled as coloured noise through a filter with transfer function

$$n(t) = \frac{C(q^{-1})}{D(q^{-1})}e(t)\,, \tag{2}$$

where $e(t)$ is uncorrelated (white) noise with zero mean and C, D are monic polynomials in the backward shift operator q^{-1}. A 'default' choice to remove the steady-state control offsets is $n(t) = \frac{1}{1-q^{-1}}e(t)$ [14]. However, a higher performance is achieved by using an 'intelligent' disturbance model [15], designed to suit the type of disturbance. Using the generic process model (1), the predicted values of the output are

$$y(t+k|t) = y_{base}(t+k|t) + y_{opt}(t+k|t)\,, \tag{3}$$

where the contributing terms are:

- $y_{base}(t+k|t)$ is the effect of the past inputs $u(t-1), u(t-2)\ldots$, a future base control sequence $u_{base}(t+k|t)$ that can be the last used input and the predicted disturbance $n(t+k|t)$.
- $y_{opt}(t+k|t)$ is the effect of the optimizing control actions $\delta u(t|t), \ldots, \delta u(t+N_u-1|t)$, with $\delta u(t+k|t) = u(t+k|t) - u_{base}(t+k|t)$, in a control horizon N_u.

The optimized output $y_{opt}(k)\,, \forall k \in [1, 2, \ldots, N_2]$ can be expressed as the discrete time convolution of the unit impulse response coefficients $h_1, \ldots, h_{N_2}$ and unit step response coefficients $g_1, \ldots, g_{N_2}$ of the system as

$$\begin{aligned} y_{opt}(t+k|t) = {} & h_k \delta u(t|t) + h_{k-1}\delta u(t+1|t) + \ldots \\ & + g_{k-N_u+1}\delta u(t+N_u-1|t)\,. \end{aligned} \tag{4}$$

Combining (3) and (4) and writing them in vector form, the key EPSAC formulation becomes

$$\mathbf{Y} = \overline{\mathbf{Y}} + \mathbf{G}\mathbf{U}\,, \tag{5}$$

where

$$\begin{aligned} \mathbf{Y} &= [y(t+N_1|t)\ldots y(t+N_2|t)]^T\,, \\ \overline{\mathbf{Y}} &= [y_{base}(t+N_1|t)\ldots y_{base}(t+N_2|t)]^T\,, \\ \mathbf{U} &= [\delta u(t|t)\ldots \delta u(t+N_u-1|t)]^T\,, \end{aligned}$$

$$\mathbf{G} = \begin{bmatrix} h_{N_1} & h_{N_1-1} & \cdots & g_{N_1-N_u+1} \\ h_{N_1+1} & h_{N_1} & \cdots & \cdots \\ \cdots & \cdots & \cdots & \cdots \\ h_{N_2} & h_{N_2-1} & \cdots & g_{N_2-N_u+1} \end{bmatrix} \tag{6}$$

Then, the control effort, U, is optimized by minimizing the cost function:

$$\sum_{k=N_1}^{N_2} \left[r(t+k|t) - y(t+k|t)\right]^2\,. \tag{7}$$

Note that (7) can be extended to alternative cost functions as described in [13]. The horizons N_1, N_2 and N_u are the design parameters and $r(t)$ represents the desired trajectory [16].

The cost function (7) can be represented in its compact matrix notation as follows:

$$(\mathbf{R}-\mathbf{Y})^{\mathbf{T}}(\mathbf{R}-\mathbf{Y}) = [(\mathbf{R}-\overline{\mathbf{Y}}) - \mathbf{G}\mathbf{U}]^{\mathbf{T}}[(\mathbf{R}-\overline{\mathbf{Y}}) - \mathbf{G}\mathbf{U}]\,,$$

where $\mathbf{R} = [r(t+N_1|t)\ldots r(t+N_2|t)]^T \in \Re^{N_2}$. That can be transformed into the standard quadratic cost index

$$J(\mathbf{U}) = \mathbf{U}^{\mathbf{T}}\mathbf{H}\mathbf{U} + \mathbf{2f}\mathbf{U} + c\,, \tag{8}$$

with,

$$\begin{aligned} \mathbf{H} = \mathbf{G}^{\mathbf{T}}\mathbf{G} \quad \mathbf{f} &= -\mathbf{G}^{\mathbf{T}}(\mathbf{R}-\overline{\mathbf{Y}}) \\ c &= (\mathbf{R}-\overline{\mathbf{Y}})^{\mathbf{T}}(\mathbf{R}-\overline{\mathbf{Y}})\,, \end{aligned} \tag{9}$$

where $G^TG \in \Re^{N_u \times N_u}$.

Finally, the feedback characteristic of MPC is given by the fact that only the first optimal control input $u^*(t) = u_{base}(t|t) + \delta u(t|t) = u_{base}(t|t) + U^*(1)$ is applied to the plant and then the whole procedure is repeated again at the next sampling instant $(t+1)$, where U^* can be analytically found for the unconstrained case as:

$$\mathbf{U}^* = [\mathbf{G}^{\mathbf{T}}\mathbf{G}]^{-\mathbf{1}}[\mathbf{G}^{\mathbf{T}}(\mathbf{R}-\overline{\mathbf{Y}})]\,. \tag{10}$$

To provide a feasible track of the ZMP, a robust extension of the EPSAC controller presented in [17] was implemented. The method modifies the singular values of matrix G providing additional properties to the controller and increasing its robustness. In the present work, a brief description of the method is provided. However, readers are encouraged to review the mentioned paper for further details.

A. Robust Extension to the EPSAC Methodology

From [18] and [19] it is known that the Singular Values Decomposition (SVD) of a system contains its stability information. In the EPSAC methodology, the computation of the optimal control input $\delta u(t)$ includes the inversion of the G matrix. Consequently, the numerical stability strongly depends on whether this matrix is well-defined. In [17], the authors present a method based on the impulse response to provide a well-defined matrix G for large control and prediction horizons based on the SVD, providing robustness to the whole system. Given (6), with $N_1 = 1$ and knowing that $h_k = 0\ , g_k = 0\ \forall k < 0\ |k \in Z$ then, G is a bottom triangular matrix. The SVD representation of G is

$$G = P\Sigma V^T \tag{11}$$

where $P = [P_1, P_2, \ldots, P_{N_2}] \in \Re^{N_2 \times N_u}$ represents the left singular vectors, $V = [v_1, v_2, \ldots, v_{N_u}] \in \Re^{N_u \times N_u}$ the right

singular vectors, and $\Sigma = diag[\sigma_1, \sigma_2, \ldots, \sigma_{N_u}] \in \Re^{N_u \times N_u}$ the singular values of G [20]. From a geometrical point of view, the SVD creates a rotated hypersphere $\in \Re^{N_u}$ that belongs to the space $\Re^{N_2}$ and the corresponding σ_i $i \in [1, 2, \ldots, N_u]$ value, defines the length in each direction.

The method changes the SVD of matrix G (6) when large control horizon N_u are used. Hence, a bigger hypersphere containing the original one is generated, with softer transition between spaces and higher correlation between hyperspaces.

1) Hypersphere construction: To identify the proper hypersphere description, first, consider that the i^{th} row of G contains the impulse response for $1 \leq j \leq N_u - 1$, where $G(i,j) = 0 \, \forall \, j > i$. Using (12), the percentual magnitude of the contribution of each h_{N1} are found $\forall k \leq N_u - 1$ as

$$C_p(i) = \frac{|h_{N1} 100\%|}{\sum_{j=1}^{i} |G(i,j)|} \, . \tag{12}$$

The new matrix Σ_C is created, where the values represented by C_p are referred to the first and last components of the original Σ matrix. The approximation provides a wider hypersphere that contains the original space solution including the contributions of the impulses from time t to time $t + j$.

III. Balancing Strategies

In this work, we propose two different compliant balancing strategies and the proper integration of them, providing a complete disturbance rejection scheme. To implement each of the strategies in the biped robot, we use the corresponding sensor signals as feedback. The real states of the robot are used by the robust EPSAC controller, according to the balancing strategy that is used, generating an unsaturated control effort U^* (10). This signal is used to analytically generate the desired trajectory for the next sampling time using the simplified model of the system. Finally, the desired trajectory is mapped to the joint space through the inverse kinematics. Fig. 1 shows the control diagram of the stabilizer.

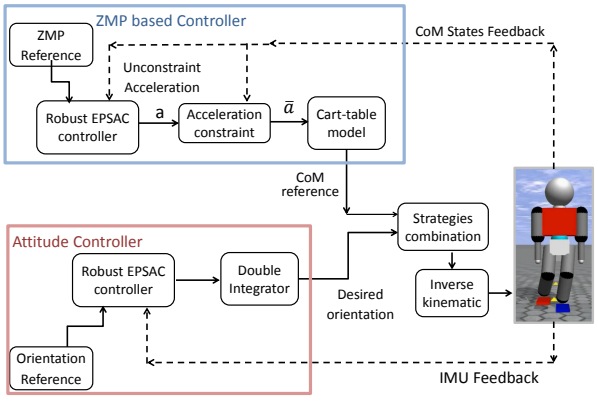

Fig. 1. Control architecture for the balancing controller.

A. ZMP based CoM controller

The ZMP provides a dynamic representation of the biped's CoM trajectory based on the actual states [10]. To model the ZMP of the biped, the cart-table model is used [10]. The cart-table models the biped as a running cart on a massless table. The cart represents the CoM position on the horizontal axis, while the table height corresponds to the CoM height. Knowing the cart's acceleration and position with respect to the bottom of the table (feet position), the ZMP is

$$x_p = x - \frac{\ddot{x}}{g} z_c \, , \tag{13}$$

whose two states space representation is

$$\begin{aligned} \dot{\mathbf{x}} &= A\mathbf{x} + BU \\ \mathbf{y} &= C\mathbf{x} + D \\ A &= \begin{bmatrix} 0 & 1 \\ 0 & 0 \end{bmatrix} B = \begin{bmatrix} 0 \\ 1 \end{bmatrix} \\ C &= \begin{bmatrix} 1 & 0 \end{bmatrix} D = [-zc/g] \, , \end{aligned} \tag{14}$$

where g is the gravitational acceleration and z_c the height of the CoM, which is assumed to be constant throughout the motion. Essentially, the dynamics is the same as that of the LIPM. However, the LIPM uses the ZMP to generate the CoM acceleration while the cart-table model uses the CoM acceleration to generate the ZMP. From the implementation point of view, the cart-table model allows the robust EPSAC controller to generate a CoM trajectory with an acceleration profile such that the resulting ZMP output tracks the ZMP reference with minimum deviation. It is desired to have a control action that generates a CoM trajectory to smoothly reject external disturbances with a compliant and human like behaviour, while keeping the ZMP within the stability margins in order to prevent the robot from tipping around the stance foot [12]. To this aim, an acceleration constraint as the one presented in [17] is considered to generate the constrained acceleration that keeps the ZMP within the stability region as:

$$\begin{aligned} \ddot{x}_{min} &= \tfrac{x - (x_{foot} + \Delta_x^+)}{z_c} g, \\ \ddot{x}_{max} &= \tfrac{x - (x_{foot} - \Delta_x^-)}{z_c} g. \end{aligned} \tag{15}$$

The proposed strategy provides a compliant CoM motion that agrees with the cart-table model, keeping the ZMP inside the support polygon. To implement this strategy on the biped, we provide the feedback to the system considering that the CoM is located at the hip x, y axes and a specific height by considering the mass distribution of the system.

B. Attitude Controller

The second balancing strategy considers the orientation of the biped around the sagittal plane. The purpose is to absorb the applied disturbances by a natural change of the orientation of the body. To achieve this, we used the double integrator model which represents the single-degree-of-freedom rotational motion [21]. By controlling the single-degree-of-freedom rotational, we generate a rotational trajectory so that the body behaves as a free rotational body

in space that rejects, with a soft dynamic behaviour, the external disturbances. With this control strategy it is possible to generate a compliant response of the rigid body that converges to the desired stable position.

The double integrator model is described as $\ddot{x} = a$ being a the desired acceleration which corresponds to the control effort. The state space representation is

$$\begin{aligned} \dot{\mathbf{x}} &= A\mathbf{x} + BU \\ \mathbf{y} &= C\mathbf{x} + D \\ A &= \begin{bmatrix} 0 & 1 \\ 0 & 0 \end{bmatrix} B = \begin{bmatrix} 0 \\ 1 \end{bmatrix} \\ C &= \begin{bmatrix} 1 & 0 \end{bmatrix} D = [0] \,, \end{aligned} \tag{16}$$

with the double integrator, a balancing strategy that depends on its dynamics and not on the model itself is obtained. The strategy allows the biped to absorb the impact by the rotation of the upper body. The use of the robust extension for the EPSAC controller provides additional advantages from the control point of view. Given the degrees of freedom for the tuning procedure it is possible to set the parameter to generate a response without overshoot but still fast. In addition, the disturbance observer (2) can be set in the range of frequencies where the disturbances have a bigger effect, i.e. cut-off frequency at 5 Hz which contains disturbances as the ones from a walking or external pushes.

The feedback is provided by the IMU sensor of the system, providing angular position and velocity measurements. These signals are applied to the controller, generating an acceleration that is evaluated in the double integrator model to provide the desired angular displacement for the next sample time. This results in the system converging to the stable position with soft dynamics provided by the double integrator model.

C. CoM Compensation

In order to integrate the decoupled strategies, we compensate for the CoM displacement caused by the rotation of the body from the orientation control strategy. We use an analytic approach for the mass compensation based on a three-mass model. The mass of the leg is equally divided and lumped to the hip and ankle respectively. Therefore, in the three-mass model, the first mass U_B is the mass of upper body (torso, pelvis, two arms and the head), the second L_B is the mass of one leg and located at the hip, and the third mass is located at the foot with the sum of the mass of one leg and two feet. Since the feet are mostly stationary during the standing balancing, so they do not affect the entire CoM of the robot.

Define $\mathbf{r_{com}} = [x, y, z]^T$ as the CoM vector of mass U_B. The objective is to compute how much the hip position needs to move to compensate for the change of CoM caused by the rotation of the U_B mass vector:

$$\Delta\mathbf{r} = -\frac{U_B}{U_B + L_B}(R - I)\mathbf{r_{com}}, \tag{17}$$

where R is the rotational matrix of the torso, and I is the identity matrix. $\Delta\mathbf{r}$ is the compensation of the hip position vector to be added to the CoM stabilization strategy (Fig. 1), such that the resulted CoM of pelvis and upper body remains the same. In other words, the rotation of the upper body does not affect the CoM of the torso and pelvis, so that the precondition of decoupling is warranted, and these two decoupled controllers can be integrated seamlessly.

TABLE I

WEIGHT DISTRIBUTION OF THE HUMANOID ROBOT COMAN.

Weight distribution		
Lower body	18.5 kg	waist and legs
Upper body	12.7 kg	torso and arms

TABLE II

DIMENSIONS OF THE HUMANOID ROBOT COMAN.

Dimensions		
Height	94.5 cm	From floor to neck
Width	31.2 cm	Measured between shoulders
Depth	20.9 cm	Measured from back to chest
Legs length	53.7 cm	From floor to hip
Leg space	14.7 cm.	Measured between ankles

IV. SIMULATION RESULTS AND PERFORMANCE ANALYSIS USING ODE

In order to demonstrate the effectiveness of the proposed strategies, a 3D model of the COMAN robot was built in the physics based simulator Open Dynamics Engine. The COMAN robot is a whole body humanoid robot with 25 Degrees Of Freedom (DOF): 13 in the upper body, including neck, elbows, shoulders and waist, and 6 DOF in each leg. The weight distribution and dimensions of COMAN are shown in tables I and II, details could be found in [22].

The different stabilization strategies were tested by applying an external disturbance at the neck of the robot. The disturbance was generated by a half sinusoid of 180 N magnitude and 0.1 s duration. In addition, we compared our results with the ones presented in [23], [24]. The active compliant stabilizer proposed firstly in [23] uses admittance control scheme to introduce compliant behavior into robot's CoM level. It takes the CoM/ZMP references and the feedback of the feet force/torque sensors as input, then generates CoM modifications according to the errors between the desired and measured resultant ground reaction torques. By transforming the references into controller's base frame, this active compliant stabilizer could also be used for stabilizing the robot and reducing the undesired impacts during walking [24].

A. Stabilizers' Independent Performances

The orientation/CoM responses of the biped after the impulsive disturbance are shown in Fig. 2 with different control strategies. As it can be seen in the orientation response, Fig. 2(a), when the ZMP based controller is activated, the orientation of the robot changes only 1.3° since this strategy only generates CoM displacement to absorb the impact and keeps the upper body upright during the impact. Instead, when the attitude controller is applied, the orientation of the

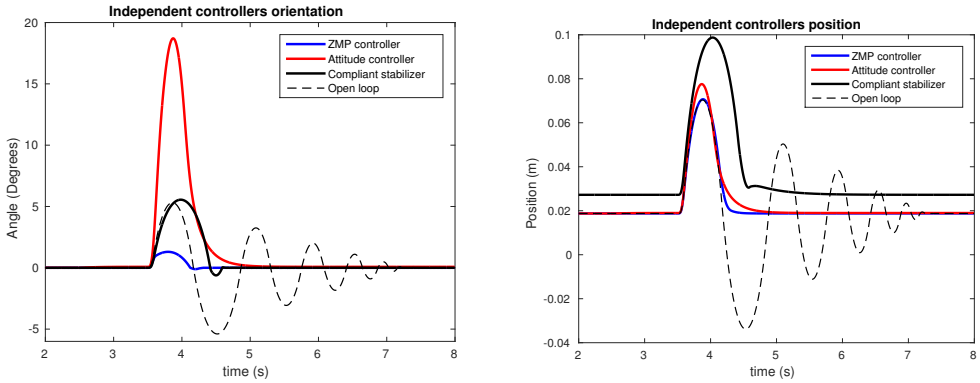

(a) Orientation response. (b) Deviation response.

Fig. 2. Independent stabilizer response against external disturbance.

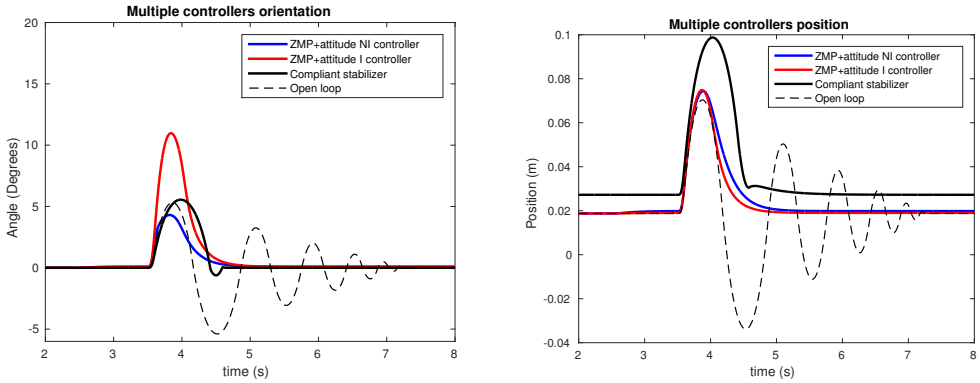

(a) Global orientation response. (b) CoM deviation response.

Fig. 3. Orientation stabilizer response against external disturbance.

upper body is dramatically affected since the compensation is generated by the upper body bending; therefore, the impact is absorbed by a rotation of the trunk. The results obtained from the compliant controller presented in [24], show that the orientation response is slightly bigger than the one obtained from the open loop simulation. On the other hand, in Fig. 2(b), it can be seen that the CoM deviation from the ZMP based controller agrees with the natural deviation of the system, the open loop response, but the controller damps out the oscillation to stabilize the system in half cycle with respect to the open loop response. The attitude controller CoM deviation is slightly bigger, showing that the bending strategy is able to absorb the impact while the CoM is kept within the stability region. Different from the compliant controller, our controller does not have offset respect to the initial standing posture. The compliant stabilizer response has a bigger CoM deviation and its settling time is 1.7 s, while for the ZMP based controller, it is 0.8 s and 1 s for the attitude one. It can be also observed that the compliant stabilizer's orientation response at 5 s has an undershoot in Fig. 2(a), which is reflected at the CoM deviation and affects the smooth recovering. Our strategies, instead, present a smooth balancing recovery after the same impact.

B. Multiple Stabilizers' Performances

In order to have a cooperative behaviour of the strategies and to increase the balancing effectiveness, it is desired to applied both controllers simultaneously. In Fig. 3, we present the responses of the robot after an impulsive disturbance when both ZMP/attitude stabilizers are simultaneously implemented using the CoM compensation methodology (I) or not (NI).

As shown in Fig. 3(a), without introducing the CoM compensation methodology, the NI controller's maximum orientation response after impact is $4.2°$, which is between the only ZMP based controller case ($1.3°$) and the only attitude controller case ($18.6°$) in Fig. 2(a). This happens because the ZMP based controller considers the upper body rotation as a disturbance and tries to compensate it. It should be noted that the the maximum orientation change is still less than the open loop response ($5.2°$). The CoM deviation response in Fig. 3(b) agrees with the one using only the attitude controller in Fig. 2(b), which is also much smaller than the compliant stabilizer response.

Meanwhile, the I controller, which integrates the ZMP and attitude controller by the CoM compensation presented in Section III-C, also shows its responses after the same impulsive disturbance in Fig. 3. Its maximum orientation response ($10.9°$) is bigger then both the ones of compliant

stabilizer ($6.7°$) and the NI controller ($4.2°$). From the orientation point of view, the I controller is more compliant by rotating the upper body more to absorb external impact compared to NI controller. On the other hand, the CoM deviation response of the integrated controller is similar to the one of NI controller, and is smaller than the compliant stabilizer response as well. It could be also seen that the responses of I controller are smooth and continuous and there is no undershoot during the recovery phase. The CoM settling time of I controller is about 1 s, which is faster than the NI controller but more gentle then the stabilizers' independent responses in Fig. 2.

Therefore, by the integrating two independent stabilization strategies, we realized compliant behaviours after external disturbance utilizing CoM deviation and body rotation, and also achieved more acceptable settling time after the disturbance. Compared with the responses of an existing compliant stabilizer, the proposed strategies demonstrated their effectiveness with shorter settling time, smoother recovering and less CoM deviation.

In addition, we also evaluate the performance of the stabilizer when a constant but soft force is applied to the biped. In this simulation we introduce a disturbance of 73 N for a period of 1 s. It can be seen in Fig. 4 that the response of the postural inclination and the CoM deviation remains around the desired stable posture with maximum values of $1.76°$ and 0.0177 m respectively. Conversely, when no balancing control is used, the biped falls. The experiment shows that in this case an ankle like strategy naturally emerges from the proposed balancing strategies. It is important to remark that the proposed strategy does not include a switching policy that changes between different balancing strategies, but the different responses naturally emerge from the controller. Fig. 5 shows the performance of the robot with (Fig. 5(a)) and without (Fig. 5(b)) the balancing stabilizer. The disturbance was generated by a ball of 2 kg impacting at a horizontal velocity of 5 m/s. The integrated balancing stabilizer allows the robot to absorb the impact and restore the stable position of the robot. It can be seen that the upper body rotates forward, while the hip moves back with respect to the feet position, providing the desired performance. Conversely, when no control is used, the applied impact results in the robot tipping over and the balance cannot be recovered, hence, the robot falls. With the proposed balancing strategy, a performance similar to the ankle strategy naturally emerges when a soft and continuous disturbance is applied. When the disturbance is stronger and fast, a performance similar to the ankle plus hip strategy is obtained. Though the lying principles are different from humans, the performance is comparable to human response against pushes.

The simulation video could be found online[1].

V. Conclusions

We propose two different balancing strategies that are integrated in order to provide stability to bipeds. The strategies show compliant responses that reject external disturbances with a soft response. It was shown that the balancing performance of the single strategies increases when there are properly integrated. The simulations results also show significant improvements in rejection of external disturbances compared to an existing compliant stabilizer.

The use of the double integrator model for the rotational balancing control and the cart-table model for the CoM displacement control make the strategies portable to other bipeds, since the considered dynamics depend only on the CoM height and the weight distribution of the robot, which are well known parameters. In addition, the required feedback signals are provide by the IMU and from the CoM states estimation that are, in general, available in humanoid robots.

We conclude that the proposed techniques and their integration produce a improved compliant balancing response for bipeds against external disturbances.

[1] https://www.youtube.com/watch?v=u4EYh9Cj0MM

References

[1] Z. Li, C. Zhou, N. Tsagarakis, and D. Caldwell, "Compliance control for stabilizing a humanoid on the changing slope based on terrain inclination estimation," *Autonomous Robots*, pp. 1–17, 2015.

[2] C. Ott, M. Roa, and G. Hirzinger, "Posture and balance control for biped robots based on contact force optimization," in *IEEE-RAS International Conference on Humanoid Robots*, Oct 2011, pp. 26–33.

[3] Y. Kanamiya, S. Ota, and D. Sato, "Ankle and hip balance control strategies with transitions," in *IEEE International Conference on Robotics and Automation*, May 2010, pp. 3446–3451.

[4] M. Raibert, *Legged Robots That Balance*. Cambridge, Massachussetts: MIT Press, 1986.

[5] B. Stephens, "Push recovery control for force-controlled humanoid robots," Ph.D. dissertation, The Robotics Institute Carnegie Mellon University, Pittsburgh, Pennsylvania, USA, 2011.

[6] D. N. Nenchev and A. Nishio, "Ankle and hip strategies for balance recovery of a biped subjected to an impact," *Robotica*, vol. 26, pp. 643–653, 2008.

[7] A. Nishio, K. Takahashi, and D. Nenchev, "Balance control of a humanoid robot based on the reaction null space method," in *IEEE/RSJ International Conference on Intelligent Robots and Systems*, Oct 2006, pp. 1996–2001.

[8] M. Morisawa, S. Kajita, F. Kanehiro, K. Kaneko, K. Miura, and K. Yokoi, "Balance control based on capture point error compensation for biped walking on uneven terrain," in *IEEE-RAS International Conference on Humanoid Robots*, Nov 2012, pp. 734–740.

[9] T. Sugihara, "Standing stabilizability and stepping maneuver in planar bipedalism based on the best com-zmp regulator," in *IEEE International Conference on Robotics and Automation*, May 2009, pp. 1966–1971.

[10] S. Kajita, F. Kanehiro, K. Kaneko, K. Fujiwara, K. Harada, K. Yokoi, and H. Hirukawa, "Biped walking pattern generation by using preview control of zero-moment point," in *IEEE International Conference on Robotics and Automation*, vol. 2, 2003, pp. 1620–1626

[11] M. Vukpbratovic and B. Boravac, "Zero-moment point - thirty five years of its life," *International Journal of Humanoid Robotics*, vol. 01, no. 01, pp. 157–173, 2004.

[12] B. Vanderborght, *Dynamic Stabilisation of the Biped Lucy Powered by Actuators with Control stiffness*, O. K. Bruno Siciliano and frans groen, Eds. Springer, 2010.

[13] R. De Keyser, *Model Based Predictive Control*. Invited chapter in UNESCO Encyclopaedia of Life Support Systems (EoLSS), vol. 83, Eolss Publishers Co Ltd, Oxford

[14] J. Maciejowski, *Predictive Control: With Constraints*, ser. Pearson Education. Prentice Hall, 2002.

[15] R. De Keyser and C. Ionescu, "The disturbance model in model based predictive control," in *Proceedings of IEEE Conference on Control Applications*, vol. 1, 2003, pp. 446–451.

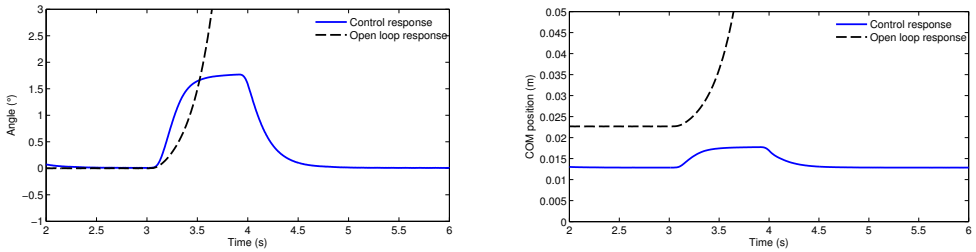

(a) Global orientation response.

(b) CoM deviation response.

Fig. 4. Simultaneous stabilizer response against soft external disturbance of 73 N during 1 s.

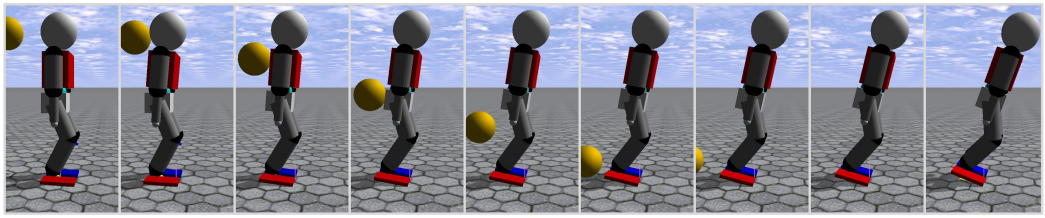

(a) Impulse response Snapshots without balancing stabilizer.

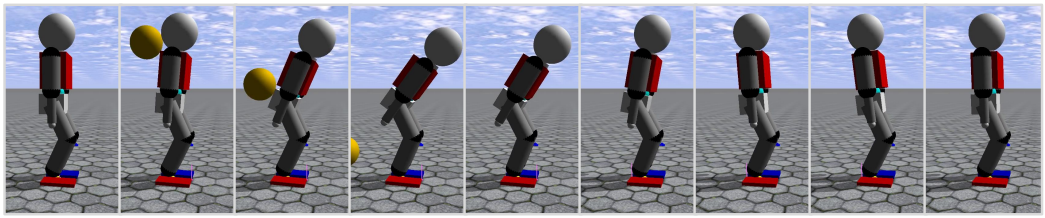

(b) Impulse response Snapshots with balancing stabilizer.

Fig. 5. Simultaneous stabilizer response against external disturbance.

[16] J. Sánchez and J. Rodellar, *Adaptive Predictive Control: From the Concepts to Plant Optimization*, ser. Prentice-Hall International Series in Systems and Control Engineering. Prentice Hall PTR, 1996.

[17] J. A. Castano, A. Hernandez, Z. Li, C. Zhou, N. G. Tsagarikis, D. Caldwell, and R. D. Keyser, "Implementation of robust EPSAC on dynamic walking of COMAN humanoid," in *19th World Congress The International Federation of Automatic Control*, Cape Town, South Africa. August 24-29, 2014.

[18] O. Rojas and G. Goodwin, "On the asymptotic properties of the hessian in discrete-time linear quadratic control," in *Proceedings of the American Control Conference*, vol. 1, 2004, pp. 239–244

[19] O. J. Rojas, G. C. Goodwin, M. M. Sern, and A. Feuer, "An SVD based strategy for receding horizon control of input constrained linear systems," *International Journal of Robust and Nonlinear Control*, vol. 14, no.13-14, pp. 1207–1226, 2004.

[20] C. Moler, *Numerical Computing with MATLAB*, E. edition: The MathWorks Inc., Ed. Print edition: SIAM, Philadelphia, 2004., 2004.

[21] V. Rao and D. Bernstein, "Naive control of the double integrator: a comparison of a dozen diverse controllers under off-nominal conditions," in *Proceedings of the American Control Conference.*, vol. 2, Jun 1999, pp. 1477–1481

[22] N. G. Tsagarakis, S. Morfey, G. Medrano Cerda, L. Zhibin, and D. G. Caldwell, "Compliant humanoid COMAN: Optimal joint stiffness tuning for modal frequency control," in *IEEE International Conference on Robotics and Automation*, 2013, pp. 673–678.

[23] C. Zhou, Z. Li, J.A. Castano, J, H. Dallali, N. Tsagarakis, and D. Caldwell, "A passivity based compliance stabilizer for humanoid robots," in *IEEE International Conference on Robotics and Automation*, May 31-June 7, 2014, pp.1487,1492.

[24] C. Zhou, Z. Li, X. Wang, N. Tsagarikis and D. Caldwell, "Stabilization of bipedal walking based on compliance control," *Autonomous Robots*, pp. 1–17, 2015.